

Electric Vehicle Application Based Fuzzy with Vector Control Controlled High Speed SRM

Prof. S.M. Bang^a, Prof. P. P. Panchbhai^b, Ms. Nikita Manwatkar^c, Mr. Aman Bangale^d

^a Associate Professor, Department Of EEE, J D College of Engineering & Management, Nagpur

^b Assistant Professor, Department Of EEE, J D College of Engineering & Management, Nagpur

^{c, d} Student, Department Of EEE, J D College of Engineering & Management, Nagpur

Abstract: When used to an electric vehicle (EV), a high-speed motor is a practical means of achieving motor reduction. Since the rotor construction of a switched reluctance motor (SRM) is both simple and sturdy, this kind of motor may be used for high-velocity drives. The driving concept is effective, although it causes significant vibration and noise. Torque controllers are notoriously difficult to build because of the complexity introduced by traditional methods of current excitation. It has been suggested that SRM drive may benefit from the fuzzy with vector control in order to get over these issues. In the high-speed drive, vector control has not yet been implemented on the SRM. In this article, fuzzy control is used to clarify the optimal drive conditions—including switching frequency and bus voltage—for operating the SRM in the high-speed range. Fuzzy with vector control is proven to be able to drive the proposed SRM in the high-speed area, allowing for minimum vibration to be achieved.

Keywords: High-speed drive, Fuzzy logic, and vector control are some of the terms used in the index.

1. Introduction

One of the energy-saving techniques that has gained popularity is the use of electric vehicles (EVs). A motor system must be downsized for electric vehicle traction motors in order to reduce electric power consumption while maintaining usable space in the motor room. Increasing the rotational velocity of a motor is one strategy for reducing its physical size [1]. Motor output power is measured as the ratio of torque to motor rotational speed. Increasing the rotational speed achieves the downsizing goal while maintaining the same output power. Because of its high torque density and efficiency, Permanent Magnet Synchronous Motors (PMSMs) with rare earth magnets are a good example of the kind of traction motor used in EVs. PMSMs, however, have a few drawbacks. The rotor's high production cost is justified by the use of rare earth elements in its construction. Additionally, the poor mechanical strength owing to the permanent magnet in the rotor restricts the high speed drive. It was hoped that Switched Reluctance Motors (SRMs) would replace permanent magnet synchronous motors (PMSMs) [2]. Only the iron core and the winding are used in the construction of SRMs, which have a prominent pole structure in both the stator and the rotor. Therefore, SRMs are well-suited for driving in the high-speed sector because to their simple and strong construction. By spinning at high speeds, they are able to reduce the size of the motor while maintaining a high output power. That's why many have reported several SRMs for the traction motor. Low-iron-loss steel, 0.1 mm thick high-silicon steel was utilised in the design of the SRM to attain the same dimensions as the PMSM found in the second-generation Toyota Prius [3] in terms of high efficiency, high torque density, and 50 kW output power from 1200 to 6000 r/min. By operating in a higher percentage of the high speed area (30,000 rpm) than PMSMs, the 80 kW SRM equipped with amorphous steel sheet for achieves the high output power and the reduction of motor volume. The usage of amorphous steel sheets may also reduce iron loss, leading to increased efficiency [4]. It has also been suggested that in-wheel EVs make use of a 12/26 pole SRM with a high specific torque [5]. Because the end-winding volume and copper loss can be reduced using the SRM's concentrated-winding configuration, the motor may be made smaller without sacrificing efficiency. However, the usual manner of driving causes SRMs to suffer from a number of drawbacks. In most cases, the unipolar current is used to power SRMs. By applying the hysteresis control or the voltage single pulse drive, the current excitation begins around the location when the rotor pole begins to align with the stator pole and maintains a consistent level. Then, it is removed just before the rotor pole and stator pole are perfectly aligned. As a result, the SRM drive often employs the use of the discontinuous unipolar current excitation. Large vibration and acoustic noise in the SRMs are caused by the current excitation being abrupt. In particular, the significant vibration is caused by the sudden shift in radial force between the rotor pole and the stator pole when the voltage is abruptly cut [6][7]. There have been reports on the best driving technique to minimise vibration [8], [9]. Torque controller design is made much more challenging by the complexity introduced by unipolar current excitation. Turn-on angle, turn-off angle, and current chopping level are only a few examples of controllable factors that must be optimised simultaneously [10, 11]. To meet the requirements of torque, good motor efficiency, a broad driving range, and low vibration in variable speed applications, these characteristics must be optimised for each drive state. A vector control for SRM has been suggested as a solution to these issues [12, 13]. Unipolar excitation current in SRM's vector control is a sinusoidal current with a DC offset supplied to each circuit. Both direct current and alternating current make up the excitation current. Because of the presence of these parts, the SRM may be driven in the same manner as traditional AC machines by virtue of the virtual rotor

flux and revolving stator field they produce. Evidence also suggests that the SRM's vibration and acoustic noise may be mitigated using vector control's use of continuous current excitation. Because the bus voltage, switching frequency, and inverter specification to realise the vector control in high speed drive have not been clarified, the vector control has not been applied to the SRM driven in the high speed area. This study elucidates the driving conditions required for implementing fuzzy with vector control of the SRM in a high-speed drive, including the bus voltage and switching frequency. Experiments further show that the suggested SRM, when operated in the high-speed area using fuzzy with vector control, is able to achieve both high output power and minimal vibration. The ultimate goals are to test the effectiveness of fuzzy with vector control in operating a 12-slot, 8-pole SRM capable of a maximum rotational speed of 50,000 rpm and an output power rating of 85,000 watts. However, the simulation environment restricts the maximum rotation speed to 20000rpm. The 8-pole 12-slot SRM driven at 50,000 rpm and the 20-pole 30-slot SRM operated at 20,000 rpm have the same electrical frequency, hence this research suggests the latter and evaluates its performance in vector control.

2. Literature Survey

Electric, Hybrid Electric, and Plug-In Hybrid Electric Vehicles: 2.1.1 Power Electronics and Motor Drives (2008) Ali Emadi, Young Joo Lee, and Kaushik Rajashekara are the authors. In order to satisfy the needs of increasing electric loads, this article emphasises the significance of power electronics as an enabling technology for the creation of environmentally friendly cars and the introduction of innovative electrical designs. For AC motor drives, 2.1.2 Unified Direct-Flux Vector Control was released in 2011. This work was written by Gianmario Pellegrino and Paolo Guglielmi. In this study, we provide a direct flux vector control system that works well with sine wave motors. The stator flux coordinates are used by this drive controller. The direct voltage component controls the stator flux amplitude, whereas quadrature current component controls the torque. All the motors utilise the same control hardware, and their software is almost identical with the exception of the magnetic model used for flux estimate at low speeds. Design Examples of Induction and Permanent Magnet Synchronous Motor Drives for Electric Vehicle Applications, 2.1.3 (2012). Gianmario Pellegrino and Alfredo Vagati authored the work. In this research, three traction motors are compared using the same vehicle specification in terms of efficiency (with the same inverter size and stack dimensions) and output power. Taking into consideration harmonic losses, core saturation, impacts of operating temperature, and skewing, a finite element is introduced and validated on all three motor drives. By tallying up the energy used throughout a typical driving cycle, we can evaluate the pros and downsides of each of the three motor drives. Using a generalized predictive control algorithm for the motor drive of an all-electric vehicle (2014) 2.1.4 Aleksej Kiselev and Alexander Kuznetsov are the authors. In this research, we describe the generalized predictive control technique for managing a permanent magnet synchronous motor in an all-electric vehicle. The generalized predictive control's theoretical foundations are laid forth, and the CARIMA model of the permanent magnet synchronous motor is derived. The generalized predictive control method may be improved for electric vehicles by taking into account the voltage restrictions imposed by the battery.

3. DC-DC Converters

Applications for this high-voltage step-up DC-DC converter include battery backup systems for uninterruptible power supply, fuel cell energy conversion systems, solar-cell energy conversion systems, and vehicle lighting. With a high effective duty ratio, a dc-dc boost converter may theoretically achieve a high step-up voltage. However, the influence of power switches and the equivalent series resistance (ESR) of inductors and capacitors limit the step-up voltage gain in practise.

When a high step-up voltage gain at a high duty ratio is required, the typical boost converter is turned to. However, the equivalent series resistance of inductors and capacitors, as well as the diode's reverse recovery difficulty, place constraints on the circuit's efficiency and voltage gain. Because of the transformer's leakage inductance, high voltage stress, and power waste caused by the converter's active switch. A resistor-capacitor-diode snubber may be used to decrease the voltage stress on the active switch and so lessen the Voltage spike. However, doing so reduces efficiency. In order to reduce the input ripple current, converters based on the coupled inductor are created. These converters use an extra LC circuit with a connected inductor to achieve their low input current ripple.

Foundations of fuzzy logic

The quantity and diversity of fields where fuzzy logic has been used have grown substantially in recent years. Consumer electronics like cameras and camcorders are only the beginning; industrial process control and medical equipment are just a few examples of the more serious uses. You need to know what is meant by "fuzzy logic" before you can appreciate why its usage has increased.

One may use fuzzy logic in two distinct ways. As an extension of multivalve logic, fuzzy logic may be thought of as a logical system. A more general definition of fuzzy logic (FL) would include the theory of fuzzy sets, which deals with categories of things that have fuzzy bounds and where belonging is a question of degree rather than

absolute truth. From this vantage point, a subset of FL is "fuzzy logic" in the restricted sense. Fuzzy logic is conceptually and practically distinct from more conventional multi-gate logical systems, even in its narrower definition. In every way, the fuzzy logic toolkit is superb. This boosts the utility of fuzzy logic as a method for developing smart systems. Fuzzy Logic Toolbox is simple to learn and implement. Last but not least, it gives an accessible and up-to-date overview of the approach of fuzzy logic and its many uses.

Fuzzy logic is predicated on the question, "How critical is it to be absolutely correct when an approximate answer will do?"

To apply fuzzy logic to a problem, you may utilise the Fuzzy Logic Toolbox add-on for MATLAB, a technical computer programme. Fuzzy logic is an interesting field of study because it effectively balances the need for accuracy with the value of significance, a task that humans have been juggling for a very long time. Although the discipline of fuzzy logic as a contemporary and rigorous science is relatively new, the notion of fuzzy logic itself depends on time-tested aspects of human thinking.

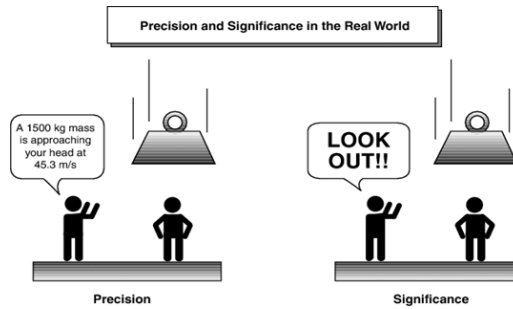


Fig.1: Fuzzy Descriptions

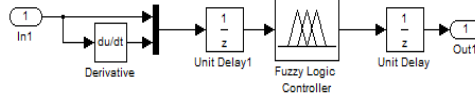


Fig.1: Fuzzy Interference System

4. Proposed System and Control Design

Proposed SRM

Fig. 1 depicts the 20 pole 30 slot SRM (model B) that fulfils the maximum rotation speed of 20000rpm, and Table I details the specifications of both this and the 8 pole 12 slot SRM (model A), which satisfies the maximum rotation speed of 50000rpm. Figure 1 and Table I demonstrate that in order to test the feasibility of control under high-speed rotation, a 20-pole 30-slot SRM was developed with the same electrical angular frequency and electrical properties as an 8-pole 12-slot SRM. Here is an expression for the electrical frequency at maximal rotation: Maximum electrical frequency f_m , maximum rotation speed N_m , and pole count P equal to $60 \pi m P f N$ (1). According to the formula (1), the model A has a maximum electrical frequency of 6.67kHz. To ensure that model B has the same maximum electrical frequency as model A at the same maximum rotation speed of 20000rpm, the number of poles is set to 20. Their outside diameters, stack lengths, and air gap lengths are all identical among these two SRMs. In addition, as can be seen in Fig. 2, they are constructed with a nearly uniform distribution of self-inductance. This is how the torque of SRMs is written out: Output torque (T), inductance (L), electric angle (θ), and phase current (i) are represented by $T = \frac{1}{2} P L T i$ (2). As demonstrated in (2), the output torque is proportional to the number of poles when supplied with a constant current value. This means that model B has a torque that is 2.5 times that of model A. However, in order to get the same torque, the current needed by Model B is 0.63 times that of Model A. The current-torque characteristics are shown in Fig. 3. Figure 3 demonstrates that in the no magnetic saturation region of low current, model B's torque is 2.5 times that of model A while using the same current.

Controllability Of Vector Control for SRM

A. Vector control's foundational theory and the state of its controller

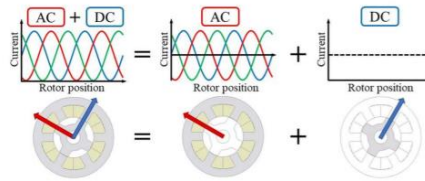


Fig. 4. Vector control of SRM.

The SRM vector control is shown in Fig. 3. The excitation current is a three-phase sinusoidal current with DC offset. The stator's magnetic field rotates because of the alternating current. The DC part generates a magnetic flux vector that rotates in response to the rotor's orientation. This vector of magnetic flux may be thought of as the magnetic flux in the rotor field. Because of this, torque is produced when the rotor's magnetic flux interacts with the stator's revolving magnetic field. The mathematical formula [9][10] describes the creation of torque during vector control of the SRM. Zero-phase and the d-q axis are used to represent the voltage equation of the equivalent SRM. where d-axis voltage (v_d), q-axis voltage (v_q), zero-phase voltage (v_0), d-axis current (i_d), q-axis current (i_q), winding resistance (R), DC component of self-inductance (L_{dc}), and self-inductance amplitude (L_{ac}) are all variables.

The DC portion of the excitation current is used to derive the zero-phase portion, as indicated in (3). The virtual rotor flux is calculated using the second term in (3)'s inductance matrix, as shown below. Where r is the virtual rotor flux, we get $0.2acRLi$ (4). Thus, the zero-phase current is demonstrated to be the source of the virtual rotor flux in (4). Then, we can write down the SRM torque as: The zero-phase and q-axis currents are equal to the rotor flux and torque currents, as described by equations (4) and (5): $2TPir$ q (5) $0.2TPLii$ ac q (6). The SRM drive's vector control system, derived from Eqs. (4) and (5), is seen in Fig. 5.

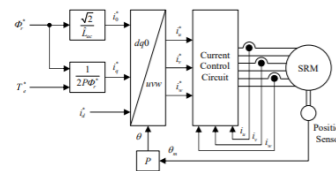


Fig. 5. Vector control system for SRM drive.

Fig. 4. Vector control system for SRM drive.

[13] explains the current controller that is being used. The present vector control controller is seen in Fig. 6. Figure 6 depicts the three components of the controller: the current PI controller, the decoupling controller, and the feedforward controller. A carrier-based PWM inverter may follow the voltage instructions from these controllers. Each axis and phase is individually controlled using a PI controller. Here is how the transfer function is written down: The transfer function, gain, and time constant of the PI controller are denoted by G_{PI} , K_c , and c in the expression $1(s) = 1 + \frac{K_c}{c s}$ (7). The controlled-SRM, thanks to the decoupling and feed-forward controllers, may be recognised as the RL circuits on the revolving reference frame. The time constant of the machine being controlled (L_{dc}/R) is chosen as the value of c to provide the desired current response at the first order. K_c , the gain, is tailored to the system's required reaction time. In this study, the controller utilised in simulations and experiments is the current controller.

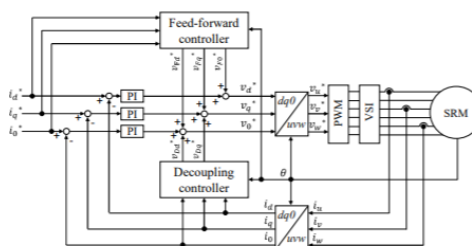


Fig. 5. The Vector Control System as it Exists Currently

B. Controllability of High-Speed Drive

When calculating the output power required and the rotation speed of 20000 rpm, the switching frequency and bus voltage are taken into account. Under the conditions of 20000 rpm rotation speed and 16.2 Nm reference torque, the simulation assesses the current waveform and the torque waveform for the switching frequency. Figure 7 depicts the switching frequency current and torque waveforms. Total harmonic distortion (THD) and current ripple ratio (CRR) are determined when the switching frequency is altered as follows (9): $THD = CRR = I_1 / THD$. The actual values of the harmonic currents at each rank are given in. Maximum current amplitude (i_{max}), lowest current amplitude (i_{min}), and average current amplitude (i_{ave}) are denoted by i_{max} , i_{imin} , and i_{ave} , respectively. Increasing the switching frequency decreases the THD and the current ripple ratio. Since iron loss in a high-speed drive rises in response to harmonic fluxes, minimising THD is essential.

5. Simulation Results

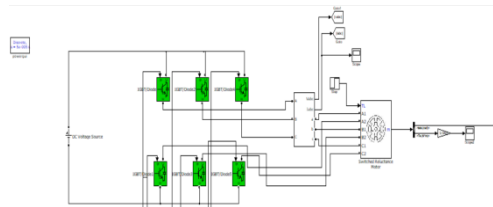


Fig. 6. Proposed Simulation Diagram

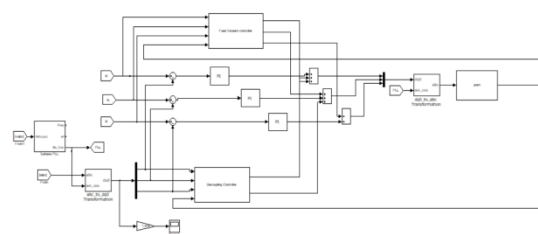


Fig. 7. Control Design

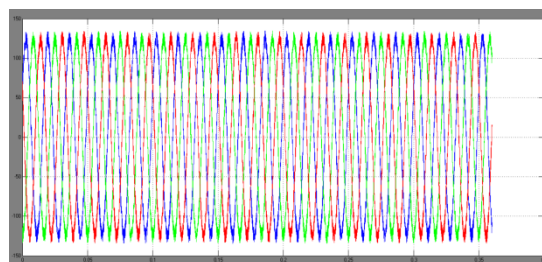


Fig. 8. SRM Input Current

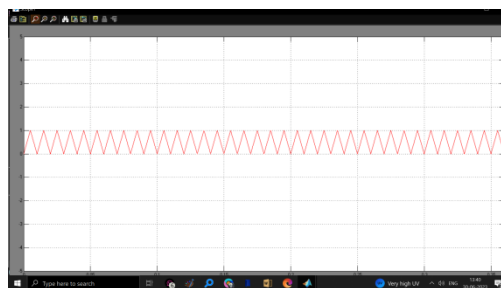


Fig. 9. d-axis, q-axis, zero-phase current

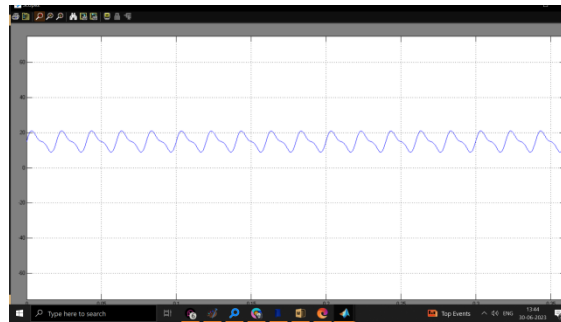


Fig. 10. Torque

6. Conclusion

We designed and tested a 20-pole 30-slot SRM driven at 20000rpm to offer vector control to the SRM in the high-speed drive. The electrical angular frequency of this SRM is the same as that of an 8-pole, 12-slot, 50000rpm SRM. By utilizing a SiC inverter with a 200kHz switching frequency, the recommended motor was able to attain the necessary torque and output power levels in the fuzzy with vector control. The simulation confirmed that the proposed SRM can be driven with fuzzy with vector control at its maximum rotation speed of 20000 rpm. Put otherwise, this suggests that the 8-pole 12-slot SRM can be used with vector control to operate at a speed of 50,000 rpm. Ultimately, it was demonstrated that the fuzzy with vector control greatly minimizes the vibration of SRM at the high-speed area when compared to the traditional single pulse drive.

References

- [1] M. Besharati, J. Widmer, G. Atkinson, V. Pickert, Jamie Washington: "Super-high-speed switched reluctance motor for automotive traction", in Proc. of IEEE Energy Conversion Congress and Exposition (ECCE), pp.5241-5248, Sept. 2015.
- [2] Earl W. Fairall, Berker Bilgin, Ali Emadi : "State-of-the-Art High-speed Switched Reluctance Machines", IEEE International Electric Machines and Drives Conference (IEMDC), pp.1621- 1627, May 2015.
- [3] A. Chiba, K. Kiyota, N. Hoshi, M. Takemoto, S. Ogasawara, "Development of a Rare-Earth-Free SR Motor with High Torque Density for Hybrid Vehicles", IEEE Transactions on Energy Conversion, vol.30, no.1, pp.175-182, Mar. 2015.
- [4] K. Ueta, K. Akatsu, "Study of high-speed SRM with amorphous steel sheet for EV", in Proc. of 19th International Conference on Electrical Machines and Systems 2016 (ICEMS 2016), Feb. 2017.
- [5] S. P. Nikam, V. Rallabandi, B. G. Fernandes, "A High-TorqueDensity Permanent-Magnet Free Motor for in-Wheel Electric Vehicle Application" IEEE Transaction on Industry Application, vol. 48, no. 6, pp.2287-2295, Nov. 2012.
- [6] M. N. Answar and Iqbal Husain, "Radial Force Calculation and Acoustic Noise Prediction in Switched Reluctance Machines" IEEE Transaction on Industry Application, vol. 36, no. 6, pp.1589-1597, 2000.
- [7] Chenjie Lin and Babak Fahimi, "Prediction of Radial Vibration in Switched Reluctance Machines", IEEE Transaction on Energy Conversion, vol. 29, no. 1, pp.250-258, 2014
- [8] H. Makino, T. Kosaka, Nobuyuki Matsui, "Digital PWMControl-Based Active Vibration Cancellation for Switched Reluctance Motors", IEEE Transaction on Industry Application, vol.51, no.6, pp.4521-4530, Nov. 2015.
- [9] A. Tanabe, K. Akatsu, "Vibration reduction method in SRM with a smoothing voltage commutation by PWM", in Proc. of 9th International Conference on Power Electronics and ECCE Asia (ICPE-ECCE Asia), June 2015.
- [10] K. M. Rahman, B. Fahimi, G. Suresh, A. V. Rajarathnam, and M. Ehsani, "Advantages of Switched Reluctance Motor Applications to EV and HEV: Design and Control Issues," IEEE Transactions on Industry Applications, vol. 36, No. 1, pp. 111-121, January/February, 2000.
- [11] I. Husain and S. A. Hossain, "Modeling, Simulation, and Control of Switched Reluctance Motor Drives," IEEE Transactions on Industrial Electronics, vol. 52, no. 6, pp. 1625-1634, December 2005.
- [12] N. Nakao, K. Akatsu, "Vector control specialized for switched reluctance motor drives", Proc. of International Conference on Electrical Machines (ICEM), pp.943-949, September 2014.
- [13] N. Nakao, K. Akatsu, "Vector control for switched reluctance motor drives using an improved current controller", in Proc. of IEEE Energy Conversion Congress and Exposition (ECCE), pp.1379-1386, Sept 2014. W.-K. Chen, Linear Networks and Systems. Belmont, CA: Wadsworth, 1993, pp. 123–135.